

# The transition of chemisorbed hydrogen into subsurface sites on Pd(311)

Daniel Farías, Peter Schilbe,<sup>a)</sup> Matthias Patting, and Karl-Heinz Rieder  
*Fachbereich Physik, Freie Universität Berlin, Arnimallee 14, D-14195 Berlin, Germany*

(Received 13 April 1998; accepted 28 September 1998)

The activated transition of chemisorbed hydrogen atoms into subsurface sites on Pd(311) has been investigated by means of He-atom scattering, high resolution electron energy loss spectroscopy (HREELS), thermal desorption spectroscopy (TDS) and work function measurements. At 120 K, hydrogen exposure leads to the formation of  $(2\times 1)\text{H}$ ,  $(2\times 1)2\text{H}$ ,  $(2\times 1)3\text{H}$  and  $c(1\times 1)2\text{H}$  phases, with coverages of 0.25, 0.50, 0.75, and 1 monolayers (ML), respectively. The TDS data show three desorption states:  $\alpha$  at  $\sim 170$  K,  $\beta_1$  at  $\sim 285$  K and  $\beta_2$  at  $\sim 310$  K. Chemisorbed H atoms forming the ordered layers desorb in the  $\beta_2$  state, whereas the  $\beta_1$  is originated by H atoms located at subsurface sites. The  $\alpha$  state is originated by decomposition of layers of Pd hydride near the surface. In all four phases, long-range order disappears at  $\sim 170$  K. Heating to 220 K leads to the migration of 0.25 ML H atoms into subsurface sites *only if* the coverage of the disordered layer is greater than 0.5 ML. The HREELS data demonstrate that this behavior is caused by the occupation of different adsorption sites as a function of coverage: only fourfold coordinated sites are occupied in the  $(2\times 1)\text{H}$  and  $(2\times 1)2\text{H}$  phases, whereas threefold coordinated sites are also occupied for  $\Theta > 0.5$  ML. A surprising result is that the HREELS peaks of the surface hydrogen vibrations still exhibit significant changes once all surface sites are occupied, and saturate only after saturation of the subsurface sites. This effect presumably results from strong repulsion between H atoms adsorbed on threefold coordinated sites and subsurface H atoms located in octahedral sites. © 1999 American Institute of Physics. [S0021-9606(99)70401-0]

## I. INTRODUCTION

The absorption of hydrogen in solids is the origin of many important technological applications. Bulk metals are ideal media for safe hydrogen storage,<sup>1</sup> but it is also known that hydrogen can reduce the mechanical stability of transition metals causing material embrittlement and cracking.<sup>2</sup> Recently, a metal–semiconductor transition was found to occur upon hydrogen absorption on a palladium-covered yttrium film, which is accompanied by dramatic changes in its optical properties.<sup>3</sup> In spite of the recognized importance of these phenomena, very little is known about the first steps involved in the diffusion of adsorbed hydrogen into the bulk, even for the very often investigated model material Pd. The influence of the different crystal surfaces on these complex phenomena has been revealed in several adsorption studies performed on low-index Pd surfaces. Whereas for both the  $(100)$ <sup>4,5</sup> and the  $(111)$ <sup>6–8</sup> surfaces the rate of hydrogen uptake into the bulk was found to be very low for temperatures below 200 K, experiments performed on Pd(110) have revealed that population of subsurface sites (i.e., sites between the first and second topmost metal layers) can be enhanced by a pairing-row reconstruction of the substrate,<sup>9–12</sup> a result which is also supported by recent *ab initio* calculations.<sup>13</sup> This subsurface species constitutes an intermediate between chemisorbed and bulk dissolved hydrogen, and as a result provides a clue for a better understanding of the first steps involved in the bulk diffusion of atomic hydrogen and hy-

dride formation. In this work we provide experimental evidence for the occurrence of a similar effect on Pd(311), but driven by a very different mechanism: no pairing-row reconstruction is involved, and the key role is instead played by the coverage of the disordered H adlayers at  $\sim 220$  K.

The fcc(311) surfaces (Fig. 1) are similar to the fcc(110) surfaces, but a little more “open”: the parallel close-packed rows are separated by  $\sqrt{\frac{11}{8}} \cdot a$ , compared to  $a$  on the (110) surfaces ( $a$  is the lattice constant). However, the most interesting feature of the fcc(311) surfaces has no equivalent on the fcc(110) ones: Due to the existence of (111) and (100) microfacets [Fig. 1(a)], there are threefold as well as fourfold hollows which are distributed with equal density through the surface. This situation leads to an interesting competition in the case of adsorbates like hydrogen or oxygen, which tend to adsorb in highly coordinated sites.

Another difference between the (311) and the (110) surfaces can be seen for the location of the possible subsurface sites (Fig. 2). For the (110) surface the octahedral site is located below the twofold short-bridge site and the tetrahedral site lies below the pseudothreefold site on the (111) microfacets. For the (311) surface the tetrahedral site is located below the twofold bridge and the octahedral site lies between the second and third layers below the pseudofourfold site on the (100) microfacets. The two different highly coordinated sites together with the different arrangement of the subsurface sites should in principle affect the H-uptake mechanism. Our current investigations of the H/Pd(311) system provide evidence in favor of this statement.

Hydrogen adsorption on Pd(311) leads to the formation

<sup>a)</sup>Also at Paul-Drude-Institut Berlin, Hausvogteiplatz 5–7, D-10117 Berlin, Germany.

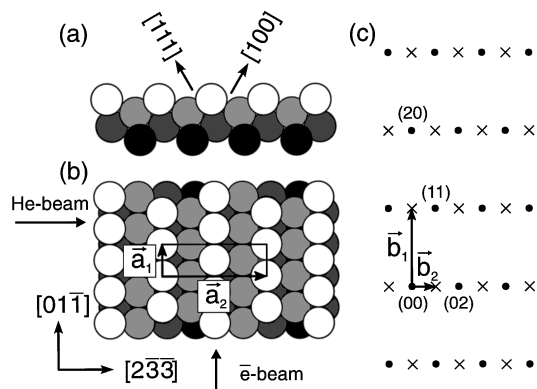


FIG. 1. (a) Side view and (b) top view of the sphere model of a fcc(311) surface. In (c) a schematic drawing of the corresponding pattern in reciprocal space is shown. Since the indices refer to a centered rectangular unit cell, only lattice points of the form  $(nm)$  with  $n+m = \text{even}$  are present in the diffraction pattern (filled circles). For Pd(311), the lattice vectors lengths are  $a_1 = 2.75 \text{ \AA}$  and  $a_2 = 9.12 \text{ \AA}$ .

of  $(2 \times 1)\text{H}$ ,  $(2 \times 1)2\text{H}$ ,  $(2 \times 1)3\text{H}$  and  $c(1 \times 1)$  phases,<sup>14</sup> with coverages of 0.25, 0.50, 0.75, and 1 monolayers (ML), respectively [the notation refers to the centered rectangular unit cell of the substrate, Fig. 1(b)]. The  $(2 \times 1)2\text{H}$  phase exhibits a mirror glide plane along  $[2\bar{3}\bar{3}]$ . As a consequence, the two hydrogen atoms in the unit cell must occupy identical sites, and form zigzag chains in the direction perpendicular to the close-packed rows.<sup>14</sup> More recently, we have shown<sup>15</sup> that heating to 220 K leads to the migration of 0.25 ML H atoms into subsurface sites *only if* the coverage is greater than 0.5 ML.<sup>15</sup> Since no evidence for any substrate reconstruction was found, it was suggested that this behavior may well be caused by the occupation of different adsorption sites at 100 K. Preliminary high resolution electron energy loss spectroscopy (HREELS) experiments performed in our group support this picture, since hydrogen was found to adsorb on the fourfold hollows at  $\Theta < 0.5 \text{ ML}$ , whereas both threefold and fourfold coordinated sites are occupied at  $\Theta > 0.5 \text{ ML}$ .<sup>16</sup>

In this work we present a detailed study on the migration of chemisorbed hydrogen into subsurface sites on Pd(311) by means of He-atom scattering (HAS), thermal desorption spectroscopy (TDS), high resolution electron energy loss

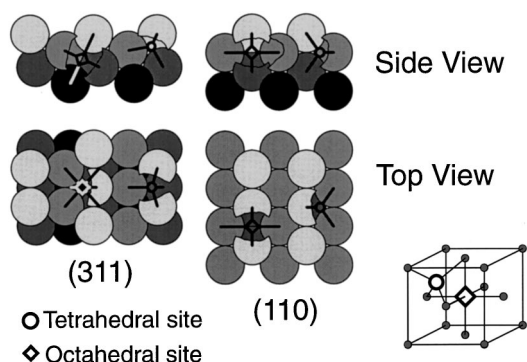


FIG. 2. Location of the subsurface sites for fcc(311) and fcc(110) surfaces. The octahedral site lies in the center of the cubic unit cell. The tetrahedral site is located in the center of a tetrahedron built up of four nearest neighbor atoms.

spectroscopy, and work function measurements. Our main goal will be to better understand the physics involved in the activated population of subsurface sites on Pd(311). A second objective concerns the desorption temperature of subsurface H species and, more generally, the meaning of the different peaks in the TDS spectra, a still controversial point also in the literature on H/Pd(110). Finally, our attempts to detect subsurface H species with HREELS demonstrate the occurrence of a new effect: the influence of subsurface H atoms on the intensity of a peak recorded in the specular direction.

## II. EXPERIMENT

The He-diffraction experiments reported here were performed with the apparatus described in detail in Ref. 17, with He pressures of 60–70 bar behind the nozzle and a base pressure in the scattering chamber of  $5 \times 10^{-11}$  mbar. The energy of the incident He beam can be varied by heating or cooling the nozzle between 115 and 800 K, corresponding to wavelengths between 0.91 and 0.35  $\text{\AA}$ , respectively. All data discussed here refer to a scattering geometry in which the beam impinges against the (111) facets, perpendicular to the close-packed rows of the Pd(311) substrate [Fig. 1(b)]. Hydrogen and deuterium exposures are given in langmuir ( $1 \text{ L} = 1 \times 10^{-6} \text{ Torr s}$ ) and are corrected with the proper gauge sensitivity factors.

The HREELS chamber is equipped with an ELS22 spectrometer, low-energy electron diffraction (LEED) optic and ion gun. The sample can be cooled down to 95 K and heated by a resistant heater. The base pressure of the apparatus was  $3 \times 10^{-11}$  mbar and the residual gas contained (like in the He diffraction chamber) mostly hydrogen with traces of CO, CO<sub>2</sub>, and H<sub>2</sub>O. HREELS spectra were taken in specular geometry at a primary energy of 4 eV and an energy resolution of 6–8 meV with count rates of the specular reflected elastic beam of  $10^4 - 5 - 10^5$  cps. The sagittal plane was arranged parallel to the rows of the Pd(311) surface [Fig 1(b)]. The recording time of the spectra was about 6 min. The cleanliness of the surface was checked by LEED and HREELS. We checked regularly for adsorption of CO from the residual gas, since it is well known that hydrogen and CO strongly interact on many surfaces.<sup>18</sup>

The Pd(311) sample was cut from a single-crystal boule after alignment by x-ray diffraction to  $\pm 0.3^\circ$  and subsequently mechanically polished. The clean surface was prepared in the ultrahigh (UHV) chamber by extended cycles of Ne<sup>+</sup> sputtering (1.0 keV, 700 K,  $P_{\text{Ne}} = 5 \times 10^{-5}$  mbar) and high-temperature treatments in oxygen and hydrogen. The presence of surface carbon on Pd cannot be ruled out by means of Auger spectroscopy, due to the overlap of the carbon peak at 272 eV with the Pd  $M_{4,5}N_{2,3}N_{4,5}$  Auger transition, and therefore some alternative ways are necessary, as discussed by He *et al.* for Pd(110).<sup>19</sup> A more careful analysis revealed that the segregation rate of carbon from the bulk becomes important at temperatures above  $\sim 650 \text{ K}$ . Accordingly, a carbon-free surface could be prepared only for temperatures in the range 100–600 K, which was considered sufficient in order to investigate H<sub>2</sub> adsorption at low temperatures. Further details on the surface cleaning procedure

can be found elsewhere.<sup>14,15</sup> The work function measurements reported in Sec. III B were performed by using a piezoelectrically driven Kelvin probe.

### III. RESULTS

#### A. The chemisorbed H phases

Figure 1(b) shows a top view of the Pd(311) surface with the centered unit cell we use for describing our results; the lattice vectors lengths are  $a_1 = 2.75 \text{ \AA}$  and  $a_2 = 9.12 \text{ \AA}$ . The corresponding lattice in reciprocal space is shown in Fig. 1(c). Note the systematic absence of reciprocal lattice points (nm) with  $n + m = \text{odd}$  in the diffraction pattern of the clean surface, due to our choice of the centered unit cell in direct space. Hydrogen exposure at 120 K leads to the formation of four ordered layers:  $(2 \times 1)\text{H}$ ,  $(2 \times 1)2\text{H}$ ,  $(2 \times 1)3\text{H}$  and  $c(1 \times 1)$ .<sup>14</sup> The first ordered structure appears after exposure to  $\sim 0.09 \pm 0.02 \text{ L H}_2$ , where the error bars result from our error of  $\pm 20\%$  in the gauge readings. Since a coverage of 0.25 ML would be reached after exposure to 0.07 L with sticking coefficient unity, we conclude that the coverage of this phase is exactly 0.25 ML and that the initial sticking coefficient lies between 0.7 and 1 [note that 0.25 ML is actually the lowest coverage consistent with the observed  $(2 \times 1)$  periodicity]. This conclusion is also based on a comparison with results obtained in a separate experiment for H adsorption on Ni(110). On this surface, a coverage of 0.33 ML [corresponding to the first  $c(2 \times 6)$  phase, Ref. 20] should be reached after exposure to 0.13 L, very close to the 0.15 L required in the experiment on Ni(110). Taking into account the error in the gauge readings, this means that the initial sticking coefficient lies between 0.7 and 1, in agreement with most experimental studies on H/Ni(110).<sup>21</sup> This supports our coverage assignment on Pd(311), and means that there is just one hydrogen atom per unit cell in the  $(2 \times 1)\text{H}$  phase.

Diffraction experiments give information on both the dimensions of the unit cell via the angular location of the diffraction peaks and the distribution of the scattering centers within the unit cell via the intensity distributions in the spectra. Because of the low energies used (10–200 meV), He atoms probe the topmost layer of surfaces in an absolutely nondestructive manner, and are equally applicable to insulators, semiconductors, and metals. This makes HAS a powerful tool for investigating the adsorption of hydrogen and weakly bonded adsorbates such as water and polar molecules.<sup>22</sup> A more exact characterization of the hydrogen overlayers can be obtained by recording the intensity of different diffraction beams as a function of  $\text{H}_2$  exposure. Such a plot is shown in Fig. 3 for two in-plane beams: the specular and the (01). Diffraction beams characteristic of a  $(2 \times 1)$  structure and in particular the ones of the form  $(0n)$  with  $n = \text{odd}$  are expected to increase with the number of  $(2 \times 1)$  unit cells on the surface. Due to conservation of the scattered flux, diffraction beams arising from the substrate must exhibit extrema when ordered adlayers are formed. In the case of the  $(2 \times 1)\text{H}$  phase, the narrow range in which it exhibits optimum order is characterized by the occurrence of the first maximum of the (01) and a minimum of the specular beam.

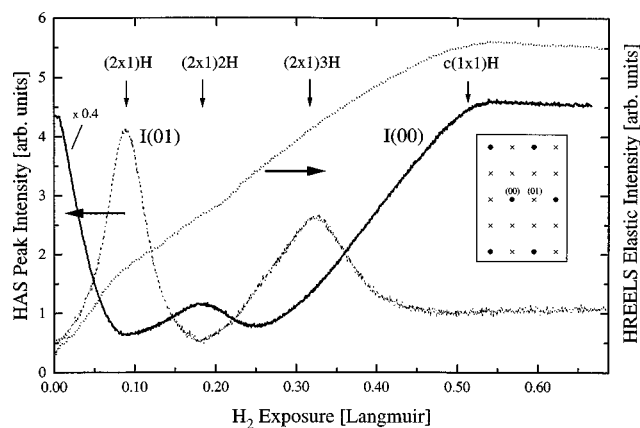


FIG. 3. Comparison of intensity variation of two diffraction beams (left scale) with that of the elastic reflected specular electron beam (right scale) as a function of  $\text{H}_2$  exposure at  $T_s = 120 \text{ K}$ . The He wavelength is  $0.57 \text{ \AA}$  and the electron beam energy  $5 \text{ eV}$ . The inset shows the reciprocal lattice pattern of the  $(2 \times 1)\text{H}$  and  $(2 \times 1)3\text{H}$  phases.

After additional  $\text{H}_2$  exposure, the (01) beam gets through a minimum while the specular beam reaches a maximum, indicating the formation of the  $(2 \times 1)2\text{H}$  phase. The new maximum of the (01) beam points to the completion of the  $(2 \times 1)3\text{H}$  phase, while the specular intensity increases steadily until it reaches the saturation value at  $\sim 0.55 \text{ L}$ , corresponding to the  $c(1 \times 1)$  phase. The existence of a glide symmetry plane in the  $(2 \times 1)2\text{H}$  phase is demonstrated by the absence of beams of order  $(0 \pm n)$  with  $n$  odd, a behavior which was observed for different scattering conditions. This means that the two hydrogen atoms in the unit cell occupy identical sites, and form zigzag chains in the direction perpendicular to the close-packed rows.<sup>14</sup>

Also shown in Fig. 3 is the exposure dependence of the elastic scattered specular beam in the HREELS experiments at a primary energy of  $5 \text{ eV}$ . Two important observations can be made on this curve. First, a change in the slope is clearly seen at  $\sim 0.1 \text{ L}$ ; second, the intensity changes much more slowly with increasing exposure from  $0.6 \text{ L}$  on. This behavior was also observed for other electron energies.<sup>16</sup> The change in the slope at  $0.1 \text{ L}$  may well be due to completion of an ordered H phase and is in accord with the observation of the  $(2 \times 1)\text{H}$  phase with HAS. The much slower change in intensity observed above  $0.6 \text{ L}$  suggests that the surface is saturated, which is again in agreement with the HAS data, where from  $0.5 \text{ L}$  on the saturated  $c(1 \times 1)$  structure was observed.<sup>14</sup> This fair agreement with the HAS curves is of the most practical importance: it confirms that, although obtained in different UHV chambers, HAS and HREELS results for a given hydrogen exposure can be directly compared with each other.

#### B. TDS and work function measurements

As can be seen in Fig. 4, three desorption states are present in the TDS data. The three lowest curves correspond roughly to the formation of the three  $(2 \times 1)$  phases. At low exposures ( $< 0.5 \text{ L}$ ) only the  $\beta_2$  state is populated. The peak maximum shifts from  $340$  to  $310 \text{ K}$  with increasing coverage, pointing to a second-order desorption process. This state originates from the chemisorbed hydrogen atoms forming the

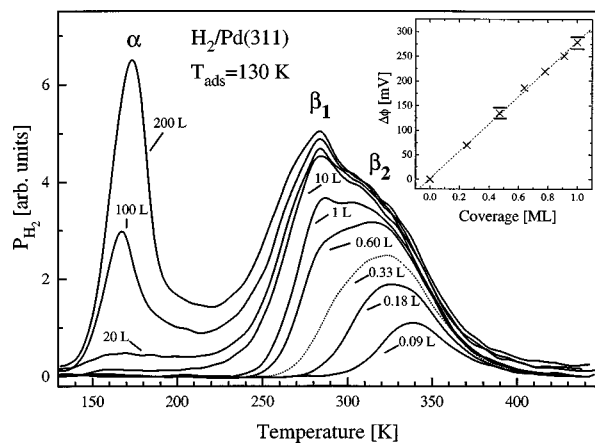


FIG. 4. Thermal desorption spectra for different  $H_2$  exposures at  $T_s = 130$  K on Pd(311). The dotted curve corresponds to desorption from the  $(2 \times 1)3H$  phase. The heating rate is 5 K/s. Inset: Work function change at 120 K as a function of hydrogen coverage (crosses). The dotted line is a least-squares fit to the crosses.

four H phases. At exposures greater than 0.5 L, the  $\beta_2$  peak broadens asymmetrically on the low-temperature side indicating the appearance of a new desorption state, which we label  $\beta_1$ . This state arises from the desorption of hydrogen atoms located at subsurface sites, as discussed in more detail in Sec. III C. Both  $\beta$  states saturate at an exposure of  $\sim 10$  L. For exposures greater than 10 L, the low-temperature state  $\alpha$  emerges at  $\sim 170$  K. It shifts to higher temperatures with increasing exposure and could not be saturated even after exposures as high as 2000 L. The common leading edge exhibited by the high-exposure curves strongly suggests a zeroth-order desorption process, which is also supported by thermal desorption (TD) spectra recorded with higher resolution by Frie *et al.*<sup>23</sup> That this peak is entirely due to H adsorption and not to the adsorption of residual water vapor was checked out using HREELS. The three desorption states showed complete isotope exchange in sequential dosing experiments, confirming that they all originate from dissociatively adsorbed hydrogen (deuterium), as expected for hydrogen adsorption on a transition metal surface. However, the  $\alpha$  state populates more slowly with deuterium than with hydrogen, whereas the  $\beta$  states are filled at the same rate after correction for the different masses of D and H. A similar behavior has been observed on Pd(110),<sup>9,12</sup> Pd(100),<sup>5</sup> and Pd(111).<sup>24</sup> As it is known that the activation energy for bulk diffusion is  $\sim 0.5$  kcal/mol lower for deuterium than for hydrogen,<sup>1</sup> the filling rate of states originated by bulk species should be smaller for hydrogen, contrary to the experimental observation. Therefore, the  $\alpha$  state should be caused by H atoms located in the first few layers below the surface. The fact already mentioned that the  $\alpha$  peak could not be saturated after exposures as high as 2000 L (whose area is equivalent to many monolayers) demonstrates that it cannot originate from H atoms located in specific subsurface sites. We believe instead that it results from the decomposition of layers of palladium hydride near the surface, as already proposed for H/Pd(110)<sup>12</sup> and H/Pd(100).<sup>5</sup> These Pd hydride layers form the hydrogen reservoir which supplies H atoms rapidly to the surface (where recombination and desorption occur), leading

to a zeroth-order desorption kinetics. Note that the isotope effect observed in the experiment is a kinetic effect, since the  $\alpha$  state does not saturate under the given experimental conditions. This effect can be explained by considering the higher diffusivity of deuterium atoms as compared to hydrogen atoms at low temperatures: Whereas H atoms remain in the near-surface region, D atoms can diffuse deeper into the bulk even at 110 K.<sup>5</sup> Only by exposure at  $T > 300$  K can the H atoms diffuse into deeper bulk regions. We have also measured TDS curves after H exposure at room temperature; the results (not shown) confirmed the presence of a broad peak around 700 K, which we interpreted as caused by bulk hydrogen. Similar results were reported by Conrad *et al.*<sup>25</sup> in their room-temperature study of H adsorption on Pd(110). The assignment of the feature at 700 K to desorption of bulk hydrogen through a diffusion-limited process is also supported by recent theoretical calculations.<sup>26</sup>

Our TDS data are qualitatively similar to the ones reported for H/Pd(110),<sup>9,12</sup> except for the absence of the  $\alpha_2$  desorption peak at  $\sim 220$  K, which is associated with the removal of the pairing-row reconstruction in the  $(1 \times 2)H$  phase. A similar behavior was also observed on Ni(110), where a sharp  $\alpha_2$  peak at  $\sim 220$  K occurs when the pairing-row reconstruction is lifted. Moreover, the pairing-row reconstructions on Ni(110) and Pd(110) are only observed after saturation of the surface, both of them having a coverage of 1.5 ML. This observation suggests that no pairing-row reconstruction is induced by hydrogen on Pd(311), at least not at coverages  $< 1$  ML. Further support for this conclusion is provided by the absence of intense diffraction spots in the LEED patterns of the  $(2 \times 1)$  phases as well as by work function ( $\Delta\Phi$ ) measurements (the inset of Fig. 4). The linear variation of  $\Delta\Phi$  with coverage in the range 0–1 ML indicates that the dipole moment remains constant until the final hydrogen structure is completed, which strongly suggests that the substrate remains unreconstructed while hydrogen adsorbs on the surface.  $\Delta\Phi$  reaches a saturation value of  $280 \pm 10$  mV after  $\sim 0.6$  L, which is close to the  $300$  mV<sup>12</sup> and  $325$  mV<sup>27</sup> reported for the H/Pd(110) system. The average dipole moment  $\mu_p$  for the adsorbate complex can be estimated by applying the Helmholtz equation. We obtain  $\mu_p = 9.3 \times 10^{-2}$  D, which is similar to  $\mu_p = 7.1 \times 10^{-2}$  D reported for H/Pd(110).<sup>28</sup> We also observed that the maximum of  $\Delta\Phi$  coincides with the saturation of the  $\beta_2$  state in the TDS spectra. This means that no work function change is associated with filling of the  $\beta_1$  state, suggesting that it originates from H atoms located at subsurface sites. Conclusive evidence in favor of this statement is given in Sec. III E.

The activation energy  $E_{des}$  for desorption of  $H_2$  from the  $\beta_2$  state can be evaluated by plotting  $\ln(2N_p T_p^2/\beta)$  versus  $1/T_p$ , where  $\beta = 5$  K/s is the heating rate,  $T_p$  the temperature at which the TDS curve shows a maximum and  $N_p$  the coverage at the maximum rate.<sup>29</sup> In this way a linear plot is obtained, as expected for a second-order desorption process. We obtain  $E_{des} = 0.86$  eV, whereby the frequency factor is  $\nu = 3.8 \times 10^7$  s. This value corresponds to an adsorption energy  $E_{ad} = 2.78$  eV. For comparison, we mention that in the case of Pd(110) the activation energy for desorption from the  $\beta_2$  state was found to be very similar,  $E_{des} = 0.87$  eV.<sup>9</sup> As-

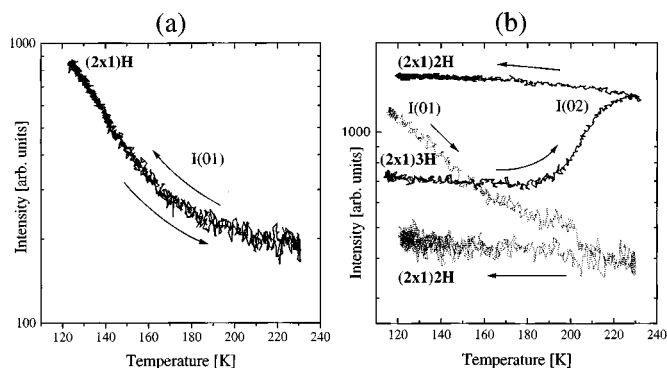


FIG. 5. The effect of temperature on diffraction beam intensities of the  $(2\times 1)\text{H}$  phase (a) and the  $(2\times 1)\text{3H}$  phase (b). The He wavelength is  $0.57\text{ \AA}$  and the angle of incidence  $40^\circ$ . Cooling down to 120 K after heating to 230 K leads to the reappearance of the  $(2\times 1)\text{H}$  phase, as demonstrated by the development of the (01) beam shown in (a). In contrast, heating the  $(2\times 1)\text{3H}$  phase to 220 K causes the migration of 0.25 ML chemisorbed H atoms into subsurface sites; spectra corresponding to the  $(2\times 1)\text{2H}$  phase are observed after cooling down to 120 K. The heating rate is 2 K/s.

suming a first-order desorption process and a frequency factor of  $\nu = 10^{13}\text{ s}^{-1}$ , a value of  $E_{\text{des}} = 0.79\text{ eV}$  results for the  $\beta_1$  state. The desorption energy associated with the  $\alpha$  peak was estimated in 0.23 eV from an analysis of the low-temperature edge in the TD spectra, following the method proposed in Ref. 30.

### C. Activated population of subsurface sites

The effect of temperature on the three  $(2\times 1)$  phases has been investigated by monitoring the development of the in-plane He-diffraction spectra as a function of temperature. These experiments have shown that, in all three phases, long-range order disappears at  $\sim 170\text{ K}$ .<sup>15</sup> These order-disorder transitions were found to be completely reversible for the  $(2\times 1)\text{H}$  and  $(2\times 1)\text{2H}$  phases upon heating to 220 K and subsequent cooling to 120 K. This is illustrated in Fig. 5(a), which shows the temperature dependence of a diffraction peak intensity from the  $(2\times 1)\text{H}$  phase. The fact that exactly the same curve is recorded in a heating-cooling cycle demonstrates the reversibility of the process. Similar results were obtained for the  $(2\times 1)\text{2H}$  phase. For the  $(2\times 1)\text{3H}$  phase, however, a very different behavior was observed: This structure transforms back into the  $(2\times 1)\text{2H}$  upon being heated to 220 K and cooling down to 120 K. More detailed information about this transition has been achieved by monitoring the changes in intensity of characteristic diffraction beams as a function of temperature. The results for the (01) and (02) beams are shown in Fig. 5(b). The (01) intensity decreases according to Debye-Waller effects up to  $\sim 165\text{ K}$ , where a change in the slope indicates that long-range order has practically disappeared. Further heating leads to a sharp rise in the (02) intensity at  $\sim 210\text{ K}$ , which coincides with the reduction of the (01) intensity to the background level, as indicated by the presence of a small descendent step at  $\sim 205\text{ K}$ . When the sample is cooling down to 120 K, typical in-plane and out-of-plane spectra of the  $(2\times 1)\text{2H}$  phase are observed. Note that, according to the TDS data of Fig. 4, no hydrogen desorbs from the surface after exposure to 0.33 L

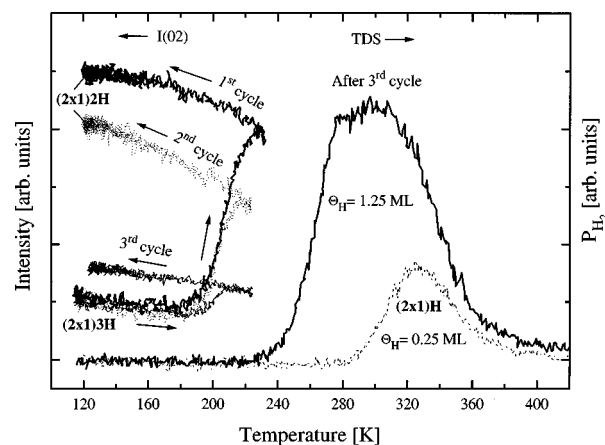


FIG. 6. The effect of temperature on the (02) beam of the  $(2\times 1)\text{3H}$  phase after performing one, two, and three thermal cycles (heating rate = 2 K/s). After completing the first two cycles, the surface was exposed to 0.15 L  $\text{H}_2$  in order to restore the  $(2\times 1)\text{3H}$  phase. The TDS curve obtained after completion of the third cycle is compared to the one corresponding to the  $(2\times 1)\text{2H}$  phase; the ratio of both areas is 5.2.

[which corresponds to formation of the  $(2\times 1)\text{3H}$  phase, the dotted curve in Fig. 4] and subsequent heating to 230 K. This demonstrates that 0.25 ML H atoms [the difference between the  $(2\times 1)\text{3H}$  and  $(2\times 1)\text{2H}$  coverages] have moved into subsurface sites.

The effect of reproducing the cycling procedure two more times is illustrated in Fig. 6. Here, the curve labeled “first cycle” describes the development of the (02) beam intensity after preparing the  $(2\times 1)\text{3H}$  phase at 120 K, heating to 230 K so that the  $(2\times 1)\text{3H}$  to  $(2\times 1)\text{2H}$  transition is complete and cooling under vacuum to 120 K. The surface was then exposed to  $\sim 0.15\text{ L H}_2$  in order to regenerate the  $(2\times 1)\text{3H}$  phase; this was actually made by monitoring the intensity of the (01) beam as a function of exposure, as it is known that completion of the  $(2\times 1)\text{3H}$  phase is characterized by a local maximum of this beam (see Fig. 3). The behavior of the (02) beam after heating to 230 K and subsequent cooling to 120 K is depicted by the curve labeled “second cycle” in Fig. 6. As becomes evident from a comparison of both curves, the  $(2\times 1)\text{3H}$  to  $(2\times 1)\text{2H}$  transition has been completed for a second time, which means that now 0.5 ML H atoms occupy subsurface sites while the same coverage is still present on the surface. Further exposure to hydrogen at 120 K leads again to the reappearance of the  $(2\times 1)\text{3H}$  phase, i.e., to an increase in the surface coverage to 0.75 ML. However, a different result is obtained by performing the cycling procedure a third time, as illustrated by the curve labeled “third cycle”: no phase transition is induced, and after cooling down to 120 K typical spectra of the  $(2\times 1)\text{3H}$  phase are observed. Also shown in Fig. 6 is the thermal desorption spectrum recorded after having completed the third cycle. Note that only the  $\beta_1$  and  $\beta_2$  states are present, which demonstrates that the subsurface H atoms desorb in the  $\beta_1$  state. The area of this curve is a factor of 5.2 larger than the area corresponding to the  $(2\times 1)\text{H}$  phase (also shown), whose coverage was assumed to be 0.25 ML. It is consistent with the general picture outlined above, in which the surface coverage amounts to 0.75 ML whereas 0.5 ML H

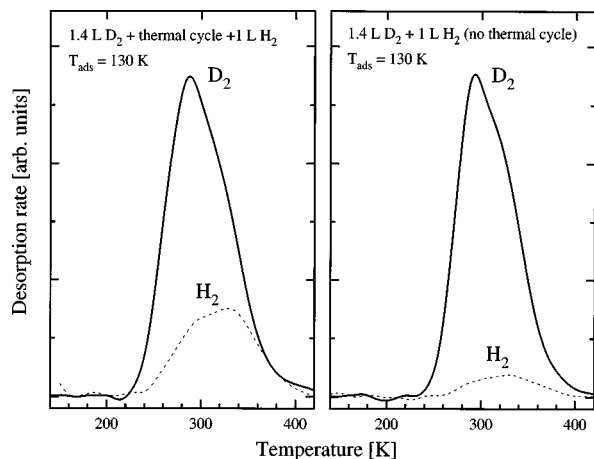


FIG. 7. Desorption spectra of  $D_2$  (the solid line) and  $H_2$  (the dashed line) after exposure to 1 L  $H_2$  on a surface preexposed to 1.4 L  $D_2$  at 130 K (right). The effect of heating the surface to 230 K prior to exposure to  $H_2$  at 130 K is shown on the left.

atoms are still present in subsurface sites. It should be mentioned that the fact that just 0.5 ML of H atoms can be accommodated between the first and second metal layers is in accordance with the results reported for H/Pd(110) by He *et al.*<sup>12</sup>

We also observed that, if a thermal cycle is performed on a phase which is intermediate between the  $(2\times 1)2H$  and the  $(2\times 1)3H$  phases (i.e., whose coverage lies between 0.5 and 0.75 ML), the  $(2\times 1)2H$  phase is obtained after cooling down to 120 K. This represents actually the most effective procedure for preparing the  $(2\times 1)2H$  phase, which due to the influence of residual gases is not very easy to obtain at 120 K. The picture is more complicated when starting with an intermediate between the  $(2\times 1)3H$  and the  $c(1\times 1)H$  phases: the spectra recorded after performing a thermal cycle reveal the existence of  $(2\times 1)2H$  and  $(2\times 1)3H$  domains on the surface. This indicates that the final coverage lies between 0.5 and 0.75 ML, suggesting that the population of subsurface sites is not as effective when the initial coverage is greater than 0.75 ML as for coverages between 0.5 and 0.75 ML.

These results clearly demonstrate that a phase transition occurs when the  $(2\times 1)3H$  phase prepared at 120 K is heated above 220 K, which is characterized by a change in the surface coverage from 0.75 to 0.5 ML. Although these results resemble in some aspects the ones reported for H/Pd(110),<sup>9-12</sup> a more detailed analysis reveals that decisive differences exist between both systems, as discussed in Sec. IV. All the results presented above were also investigated using deuterium instead of hydrogen. The only isotope effect observed concerns a shift of the subsurface-transition temperature to  $\sim 240$  K. The fact that such an effect was not observed on Pd(110) again proves the different nature of the phase transitions on the two systems (see the discussion in Sec. IV). We have also tried to distinguish surface from subsurface species by analyzing TDS data of surfaces exposed to  $H_2$  and  $D_2$  in different sequences. The results from one of these experiments are shown in Fig. 7, which illustrates the effect of thermal cycling on a deuterium-covered surface.

The clean surface was first exposed to 1.4 L  $D_2$  at 130 K in order to saturate all surface adsorption sites, and subsequently to 1 L  $H_2$ . Thermal desorption spectra of  $D_2$  and  $H_2$  from this surface are shown on the right-hand side of Fig. 7. As expected from the very low sticking probability after exposure to 1.4 L  $D_2$ , practically no  $H_2$  desorption is observed (the curves are the result of two different runs). A very different result is obtained if the deuterium-covered surface is heated to 250 K and cooled to 130 K prior to exposure to 1 L  $H_2$ . The migration of D atoms into subsurface sites leaves surface adsorption sites free, which enhances the probability of adsorption of  $H_2$  at 130 K. Hence, a significant  $H_2$  desorption peak is observed in the TDS data. Note that thermal cycling has no influence on the desorption of  $D_2$ , which causes in both cases the appearance of  $\beta_1$  peaks (originated by D atoms located in subsurface sites) and  $\beta_2$  peaks (caused by chemisorbed D atoms). A similar behavior has been observed when the opposite dosing sequence (i.e., first  $H_2$  and then  $D_2$ ) was applied.

## D. HREELS results

### 1. Subsurface hydrogen

Now the question arises whether HREELS can judge how the incorporation of hydrogen below the surface takes place and if it may be possible to observe vibrations of subsurface hydrogen atoms. Low energy electrons — as used for HREELS — penetrate some ten of angstroms in the surface when scattered from a metal surface. Therefore, they are able to excite vibrations of atoms situated below but near the surface. Due to the screening of the valence band electrons in metals, the vibrations of hydrogen atoms below the surface cannot be dipole active. The selection rules that apply for subsurface atoms are the impact scattering ones (off-specular scattering geometry) and only apply to vibrations which are antisymmetric with respect to mirror planes of the surface. The fcc(311) surface only shows one mirror plane perpendicular to the closed packed rows. The dipole scattering cross section for hydrogen above the surface is usually very low and comparable to the differential cross section in the impact scattering regime. Therefore subsurface hydrogen vibrations which lie within the mirror plane may be observed also in the specular scattering geometry. Nevertheless, the low intensity in the impact scattering regime and the obscuration of the subsurface peaks by surface vibrations make the observation of subsurface hydrogen with HREELS a difficult task. The only direct evidence of a hydrogen vibration below the surface observed with HREELS was found for the system H/Ni(111).<sup>31</sup> The assignment of a loss peak to subsurface hydrogen was based on the dependence of the peak intensity on the energy of the impinging electrons. For hydrogen in Pd no evidence for subsurface vibrations in the HREELS spectra was reported so far. For H/Pd(110), Ellis and Morin<sup>32</sup> have searched for subsurface hydrogen with HREELS. They have found no evidence of subsurface hydrogen in their spectra after exposures to 10 L  $H_2$ , nor after following the recipe of He *et al.*<sup>12</sup> Also in the specular direction they found no change of the peaks with or without subsurface hydrogen present.

TABLE I. HREELS vibration energies (in meV) previously reported for hydrogen adsorption on low-index Pd surfaces compared with the ones observed on Pd(311). Vibrations associated with symmetric and asymmetric modes are indicated by (s) and (a), respectively.

Surface	Fourfold site	Threefold site	Ref.
Pd(100)	63(s) 83(a)	...	34–36
Pd(111)	...	96(a) 124(s)	37
Pd(110)	...	98 120	32
Pd(210)	55	90	33
Pd(311)			
0.1 ... 0.4 L	56 85	94 120	16
>0.4 L	50~85	~90 126	16

## 2. Hydrogen adsorption on Pd(311)

Concerning the H/Pd(311) system, we want to first briefly discuss the HREELS results for chemisorbed hydrogen. A full discussion of the site assignment for hydrogen on the surface can be found in Ref. 16. Although a simple comparison of vibration energies between different surfaces to determine adsorption sites can be erroneous, in the present case the comparison with the low index surfaces (100), (111), (110) and the recent investigations of Muschiol *et al.*<sup>33</sup> for Pd(210) leads to a conclusive assignment of the peaks.<sup>16</sup> In Table I the vibration energies for hydrogen on Pd(311) from our previous investigation<sup>16</sup> are compared with the energies found on other Pd surfaces. In Fig. 8 spectra in specular scattering geometry for different exposures are shown. In the 0.2 and 0.3 L spectra of Fig. 8 the peak at 80–85 meV can be attributed (see Table I and Ref. 16) to the vibration parallel to the fourfold microfacet, and the peaks at 94 and 120–126 meV to the parallel and perpendicular vibrations in threefold sites.<sup>16</sup> The surface exhibits  $C_s$  symmetry so that for each adsorption site two dipole allowed vibrations are expected. The second dipole active vibration of hydrogen in the fourfold site is visible as a shoulder at 56 meV and is better resolved in the scattering geometry with the scattering plane arranged perpendicular to the closed packed rows (not shown, see Ref. 16) or in off-specular spectra (the insert in Fig. 8). The intensity of this peak in specular and off-specular geometry is similar. It is therefore not (or not strongly) dipole active. The very good agreement between the observed vibration energies with the corresponding ones on the low index surfaces makes it very unlikely that the assignment of the adsorption sites given in Ref. 16 should be wrong. Up to about 0.2 L the intensity of the peaks associated with the threefold sites is small. This means that, although occupation of threefold sites is also expected at finite temperatures, mainly the fourfold sites are occupied in the first two phases — the (2×1)H and (2×1)2H. Domination of an adsorption site at low coverages has also been reported for H adsorption on Ni(311)<sup>18</sup> and Rh(311).<sup>38</sup> From 0.2 to 1 L the threefold sites are filled until a coverage of 1 ML is reached. In the (2×1)3H phase two fourfold and one threefold site are occupied. The work function (Fig. 4) and the elastic intensities of the HAS and HREELS (Fig. 3) are not altered markedly at exposures >0.55 L, indicating saturation of the surface. The only change observable in the HREELS spectra for exposures >1 L is an increase of the

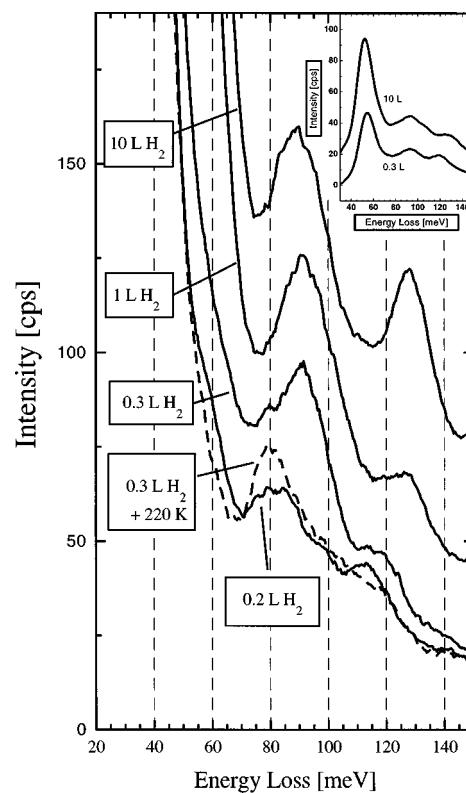


FIG. 8. Comparison of HREELS spectra from the (2×1)2H phase (the 0.2 L curve) and the (2×1)3H phase (the 0.3 L curve). The specular spectra are normalized to an elastic intensity of  $1.2 \times 10^5$  cps, which was the elastic intensity of the 10 L spectrum. The energy of the primary electrons is 4 eV and the angle of incidence  $\theta_i = 60^\circ$ . The effect of heating the (2×1)3H phase to 220 K (depopulation of threefold sites) is illustrated by the dashed curve. Spectra recorded after exposure to 1 and 10 L are also shown. The spectra shown in the inset were recorded at  $12^\circ$  off specular (with respect to the surface normal). The scattering plane was orientated perpendicular to the closed packed rows. Note the strong increase of the peak at 120 meV, which is only seen in the specular spectrum.

intensity of the 120 meV peak up to 10 L exposure. This is a very interesting effect and will be discussed in more detail below.

Above 0.3 L the peaks at 80 and 96 meV move closer together so that they are not well resolved. It should be remarked that the observed peak width results in part from the intrinsic width of the vibrations, which is on the order of 5–10 meV.<sup>39</sup> The peak at 56 meV can be seen in all off-specular spectra for high exposures. It shifts for exposures >0.2 L to 50 meV. The vibration energies of bulk palladium hydride are 96 and 56 meV for the phases  $\alpha$  and  $\beta$ , respectively.<sup>40</sup> Nicol<sup>41</sup> has observed a mode at 58 meV with neutron scattering measurements, which was assigned to subsurface hydrogen. These energies are nearly identical to the energies for the surface hydrogen, so that large changes in the spectra or new peaks are not expected when subsurface hydrogen is present. Although we have performed an extensive search for new peaks in the impact scattering region, we did not find any evidence for structures which may be caused by subsurface hydrogen. The only hint of possible subsurface hydrogen is the appearance of additional shoulders at 56 and 65 meV, which were not well reproducible and are therefore not shown here.

In this context an apparent contradiction between the HAS and HREELS results should be mentioned. In HAS a clear  $c(1\times 1)$  structure was observed for high exposures ( $>0.5$  L). The saturation coverage of the surface was determined by HAS and TDS to be 1 ML. Therefore only a single adsorption site should be occupied. This is in contrast to the findings of HREELS for high exposures, which showed two adsorption sites for the saturated phase. We think that two explanations are possible to solve this contradiction. First, there are two different domains giving rise to the  $c(1\times 1)$  structure, which differ in the occupation of threefold or fourfold sites, respectively. Since the two domains are expected to be energetically similar, the observation of one or the other structure may critically depend on the temperature. A similar effect has been recently proposed to explain the existence of two different adsorption sites on the  $c(2\times 4)4H$  phase on  $\text{Co}(10\bar{1}0)$ , on which the H atoms form zigzag chains along the metal rows. Two different domains result depending on whether fcc- or hcp-like adsorption sites are occupied.<sup>42</sup> A second explanation is based on the observation that the peak at 85 meV disappears at high exposures. The peak at 50 meV should therefore not result from hydrogen in a fourfold site. As mentioned above a subsurface vibration could also be observable in a specular scattering geometry if it is symmetric under the mirror plane. Now one can speculate if this peak results from subsurface hydrogen. The peak is not dipole active and it lies in the correct energy region. On the other hand the peak has the same or even a higher intensity as the other hydrogen peaks. This is in contrast to the expectation that peaks from subsurface vibrations should have low intensity. From our present data we cannot judge which explanation is the correct one.

### 3. Population of subsurface sites on Pd(311)

Now we turn to the investigations of the activated population of subsurface sites. In Fig. 8 the dashed curve shows a spectrum recorded after an exposure of 0.3 L  $\text{H}_2$  at 100 K and a subsequent flash to 220 K. The spectrum looks very similar to the spectrum recorded after exposure to 0.2 L. The peaks at 96 and 120 meV in the dashed curve — which indicate occupation of the threefold sites — have nearly disappeared. In fact, traces of H atoms occupying threefold sites were observed in all spectra recorded for exposures up to 0.2 L. This is in accordance with the HAS results, which showed that the  $(2\times 1)2H$  phase is best prepared after exposure to 0.3 L  $\text{H}_2$  and subsequent heating to 220 K.<sup>15</sup> Figure 9 shows a complete cycle leading to successive filling of the subsurface sites: exposure to 0.3 L  $\text{H}_2$  at 100 K [which correspond to formation of the  $(2\times 1)3H$  phase], heating to 220 K, exposure to 0.1 L  $\text{H}_2$  at 100 K, heating to 220 K. In the first step the threefold hydrogen peak at 96 meV disappears (the lowest curve). It is refilled in the second step with 0.1 L  $\text{H}_2$  (the dashed line). The resulting spectrum is very similar to the first spectrum after exposure to 0.3 L. In the last spectrum (the dotted line) the occupation of the threefold site is again strongly depleted. The residual occupation of the threefold site presumably originates from hydrogen adsorption from the residual gas, which consisted mainly of hydrogen. The observation of nearly identical spectra after heating to 220 K

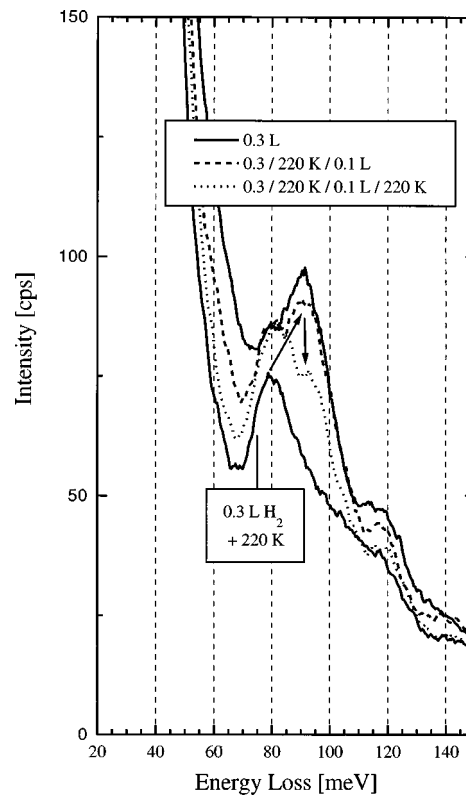


FIG. 9. The effect of reproducing the thermal cycle one more time on the HREELS spectra. The population of subsurface sites after heating to 220 K is clearly connected with a depopulation of threefold sites on the surface. Same scattering conditions as in Fig. 8.

or refilling the surface nicely resembles the behavior seen with HAS, which is summarized in Sec. III C. Experiments with a further hydrogen exposure and a following flash to 220 K were not possible because we were not able to check whether the  $(2\times 1)2H$  or  $(2\times 1)3H$  phases were prepared sufficiently well. Additional experiments with deuterium showed no conclusive results because the deuterium peaks overlap with peaks of hydrogen from the residual gas.

A remarkable effect can be seen for hydrogen exposures above 1 L (Fig. 8). The peak at 120–126 meV associated with the perpendicular vibration in the threefold site increases in intensity until it is saturated at about 10 L. The other peaks — especially the peak at 96 meV — do not change between 1 and 10 L. For exposures higher than 10 L the whole spectrum does not change any more. In off-specular spectra the intensity of the 120 meV peak does not change appreciably for exposures between 1 and 10 L, apart from shifting from 120 to 126 meV (the insert in Fig. 8). According to the interpretation of the HAS, TDS, and work function data the surface is saturated at 1 L and from 1 to 10 L the subsurface sites are filled. Thus, a higher occupation of surface sites can be ruled out. This is in accordance with the fact that the peak associated with the parallel mode in the threefold site and the off-specular intensities do not change. If occupation of threefold sites would increase for exposures  $>0.7$  L both peaks should increase in intensity. Therefore we assign the intensity increase of the 120 meV peak to the formation of subsurface hydrogen. In principle, such an interpretation seems unlikely because the screening of the con-

TABLE II. Distances between the adsorption sites and the subsurface octahedral and tetrahedral sites on Pd(110) and Pd(311).

Surface	Adsorption site	Coordination	Subsurface site	Distance (Å)
(311)	(100)	Fourfold	Octahedral	2.75
(311)	(100)	Fourfold	Tetrahedral	1.59
(311)	(111)	Threefold	Octahedral	1.95
(311)	(111)	Threefold	Tetrahedral	0.98
(110)	(111)	Threefold	Octahedral	1.12

duction band electrons should prevent an observation in the specular direction with such a high intensity and the energy does not fit the energies of bulk hydrogen in Pd. However, linear muffin-tin orbital (LMTO)-calculations performed by Henning *et al.*<sup>43</sup> have shown that for hydrogen located in the fourfold hollow sites of Pd(100), the adsorption height of hydrogen is increased from 0.11 to 0.18 Å when at the same time subsurface octahedral sites just beneath the surface are occupied. Such an increase of the binding height can easily lead to an increase of the dynamic dipole moment responsible for the intensity of the vibration peak near the specular beam. The conclusion is that the subsurface hydrogen added for exposures up to 10 L changes the binding of hydrogen in the threefold site and leads to an increase of the dynamic dipole moment. From the fact that no appreciable change in the surface work function was observed for exposures > 1 L (Sec. III B) we conclude that the change of the work function induced by the increase of the H–Pd bond length is less than 10 meV (the confidence of our  $\Delta\Phi$  measurements). In this context it is interesting to note that Nyberg and Westlund<sup>44</sup> have observed that for a CO induced dissolution of hydrogen in Pd(100) the intensity of the perpendicular vibration of hydrogen seems to increase upon filling the subsurface sites and to shift to lower energies. For exposures above 10 L the HREELS spectra do not change any more. This proves together with the arguments given above that for high exposures neither the surface hydrogen occupation nor the occupation of sites between the first and third layers change any more. For higher exposures (>10 L) we have also checked for possible contaminations of the surface with H<sub>2</sub>O or OH, which have O–H stretch vibrations in the region around 450 meV, but we have found no traces of such a contamination.

#### 4. Location of subsurface hydrogen

Now one can ask where the subsurface hydrogen is situated. The location of the subsurface sites for the (311) and the (110) surfaces is different as mentioned in Sec. I (Fig. 2). It is interesting to take a look at the distances between the adsorption sites and the subsurface octahedral and tetrahedral sites (Table II). According to the ‘‘Switendick criterion’’ hydrogen atoms in the bulk never come closer than 2.14 Å.<sup>45</sup> Furthermore, local density calculations performed in the group of Nørskov<sup>46</sup> have shown that a strong short range repulsion between H atoms exists in Pd, which prevents the occupation of one unit cell with two hydrogen atoms. Therefore, for the Pd(311) surface a tetrahedral site for the subsurface hydrogen with saturated threefold sites on the surface seems unlikely since a possible outward relaxation of the

surface together with the adsorption height of the hydrogen should add to over a 1 Å increase of the H–H distance (see Table II). The distance of an octahedral hydrogen to the threefold surface hydrogen is too small by  $\sim 0.2$  Å. This could be easily achieved by a small increase of the adsorption height and by an increase of the distances between the first layers of a few percent. The increase of the adsorption height would then be reflected by a change of the dynamic dipole moment of the hydrogen vibration perpendicular to the threefold sites. For hydrogen adsorbed on a fourfold hollow site the distance to the next octahedral site is with 2.75 Å large enough so that no influence of subsurface hydrogen on surface hydrogen in fourfold sites is expected. These considerations give a simple explanation of the observed increase of the dynamic dipole moment but only in the vibration perpendicular to the threefold adsorption site. For the H atoms shifted below the surface after heating to 220 K we do not observe a large increase of the intensity of the threefold perpendicular vibration. As already mentioned, heating leads to depopulation of the threefold sites. After refilling of the threefold sites with hydrogen, the surface coverage is with 0.75 ML low enough that subsurface H atoms can avoid the sites below a surface hydrogen. Therefore it seems natural that we did not observe any intensity increase in this case.

On the (110) surface the behavior should be different due to the different geometry of the surface layers. The octahedral site between the first and second layers lies only 1.12 Å below the pseudothreefold site. Therefore a simultaneous occupation of the threefold sites and the octahedral subsurface sites seems unlikely and a different uptake mechanism for hydrogen results.

#### E. Subsurface hydrogen and the $\beta_1$ state

Although there is general agreement in the literature about the physics involved in the interaction of H<sub>2</sub> with Pd(110), discrepancies appear when some questions related to the population of subsurface states are considered. Cattania *et al.*<sup>27</sup> interpreted the  $\alpha_1$  state in the TDS data as arising from H atoms located in subsurface or surface-near bulk regions of the crystal whereas the  $\beta_1$  state was ascribed to chemisorbed H atoms. The H/Pd(110) system was also investigated by Rieder *et al.*,<sup>10,11</sup> who suggested that the  $\alpha_1$  state is connected with H atoms located in the first few layers below the surface whereas the subsurface H atoms desorb in the  $\alpha_2$  state. In a more recent work, He *et al.*<sup>12</sup> have claimed that H atoms located at subsurface sites actually desorb in the  $\beta_1$  state while the  $\alpha_1$  state is linked to the decomposition of layers of Pd hydride near the surface. The experimental evidence presented below gives support to the last of these arguments.

We have recently demonstrated that the clean Pd(311) surface can be prepared in a (1×2) missing-row metastable structure.<sup>47</sup> This structure consists of missing-row domains in addition to unreconstructed  $c(1\times 1)$  patches and is metastable, i.e., it reverts to the clean (1×1) surface at  $\sim 370$  K. More detailed information about this phase transition was achieved by monitoring the intensity changes of some characteristic diffraction beams as a function of temperature. The

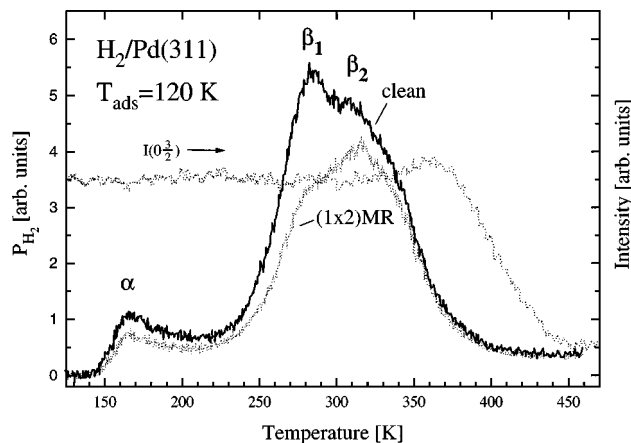


FIG. 10. Thermal desorption spectra from the clean surface (the solid line) and the  $(1 \times 2)$ MR structure (the dotted line) after exposure to 50 L  $H_2$  at 120 K. Also shown is the evolution of the  $(0 \frac{3}{2})$  beam of the  $(1 \times 2)$ MR structure as a function of temperature. The heating rate is 5 K/s.

curve obtained for the  $(0 \frac{3}{2})$  beam is shown in Fig. 10 (the data have been corrected for Debye–Waller effects). The measurements were performed with the same heating rate as the TD spectra (5 K/s), with a He-beam wavelength of 0.82 Å and an angle of incidence  $\theta_i = 40^\circ$ . The intensity remains constant up to  $\sim 340$  K where it increases slightly due to the desorption of residual hydrogen (estimated in  $\sim 0.09$  ML, Ref. 47). That these residual H atoms cannot be responsible for the induced missing-row structure has been demonstrated by measuring diffraction spectra after completing several heating–cooling cycles, as discussed in more detail in Ref. 47. The intensity decrease observed from 370 K on indicates the onset of the transition, which is completed at 450 K. The fact that the density of close-packed rows in the top layer is lower for this structure than for the clean surface actually provides a very interesting scenario to study the possible locations of the subsurface H atoms as well as the way in which they desorb from Pd(311). In effect, if we assume that H atoms occupy sites between the topmost and the third layer, it is reasonable to expect that a diminution of the number of close-packed rows present in the first layer would affect the population of such sites. In order to learn more about this point, we have investigated the thermal desorption of hydrogen from the  $(1 \times 2)$ MR structure. Figure 10 shows the curve obtained after exposure to 50 L  $H_2$  at 120 K, which is compared to the curve corresponding to the clean surface. The lower population of the  $\beta_1$  state in the case of the reconstructed surface is evident, as expected from the arguments discussed above. Note also that no noticeable changes are evidenced in the  $\alpha$  and  $\beta_2$  states. Such behavior was observed systematically for several  $H_2$  exposures. Therefore, we conclude that the subsurface H atoms desorb in the  $\beta_1$  state.

#### IV. CONCLUSIONS

The adsorption as well as the first steps involved in the absorption of hydrogen on Pd(311) have been investigated by HAS, HREELS, TDS, and work function measurements. The HAS results prove that hydrogen adsorbs dissociatively

on Pd(311) at 120 K with a high initial sticking coefficient. Hydrogen exposure leads to the formation of  $(2 \times 1)H$ ,  $(2 \times 1)2H$ ,  $(2 \times 1)3H$  and  $c(1 \times 1)H$  phases with coverages of 0.25, 0.50, 0.75, and 1 ML, respectively. The TDS data recorded after exposure to  $H_2$  at 120 K show three desorption states:  $\alpha$  at  $\sim 170$  K,  $\beta_1$  at  $\sim 285$  K, and  $\beta_2$  at  $\sim 310$  K. In all four hydrogen phases, the chemisorbed H atoms desorb in the  $\beta_2$  state. This state exhibits a second-order desorption kinetics with an activation energy for  $H_2$  desorption  $E_{des} = 0.86$  eV. Completion of the  $c(1 \times 1)H$  phase coincides with saturation of this state. The  $\alpha$  state populates slower with  $D_2$  than with  $H_2$  and is believed to originate from the decomposition of layers of palladium hydride in the first few layers below the surface. With respect to the  $\beta_1$  state, the TDS results presented in Sec. III E prove that it originates from H atoms located in subsurface sites, as also proposed for the system H/Pd(110) by He *et al.*<sup>12</sup>

In all four phases, long-range order disappears at  $\sim 170$  K. Heating to 220 K leads to the migration of 0.25 ML H atoms into subsurface sites *only if* the coverage of the disordered layer is greater than 0.5 ML. Although this behavior resembles in some aspects the ones reported for the H/Pd(110) system,<sup>9–12</sup> the results presented in our current work demonstrate that important differences exist between the two systems. On Pd(110), two ordered structures can be formed after hydrogen adsorption at 100 K: a  $(2 \times 1)$  phase (with  $\Theta_H = 1$  ML) and a  $(1 \times 2)$  phase (with  $\Theta_H = 1.5$  ML) which exhibits a substrate reconstruction of the pairing-row type.<sup>9,10</sup> This reconstruction allows the adsorption of 0.5 ML H atoms on the second Pd layer and (upon heating to 220 K) the subsequent migration to subsurface sites when the pairing-row reconstruction is lifted. On Pd(311), on the contrary, no pairing-row reconstruction is induced in any of the  $(2 \times 1)$  phases. Therefore, a different mechanism must be responsible for the activated population of subsurface sites on Pd(311). Although a detailed understanding of this mechanism cannot be achieved solely on the basis of our current results, they show clearly that at  $\sim 220$  K the more stable configuration is the one with 0.5 ML H atoms on the surface and the rest on subsurface sites. The fact already mentioned that disorder of the H adlayers precedes the activated migration into subsurface sites also suggests that an important role may be played by a partial occupation of different adsorption sites, from which migration into subsurface sites appears easier. This is confirmed by our HREELS results, which revealed that H atoms adsorb on the fourfold coordinated sites for coverages  $< 0.5$  ML. This hypothesis is also supported by the observation that the  $(2 \times 1)3H$  to  $(2 \times 1)2H$  transition is shifted to a higher temperature ( $\sim 240$  K) when deuterium is used instead of hydrogen. Such an effect was not observed on Pd(110), which underlines the different H-uptake mechanism involved on the two surfaces. Whereas on Pd(110) the transition is driven by lifting of the substrate reconstruction (which occurs at the same temperature independently of whether H or D atoms are adsorbed on the surface), on Pd(311) actual diffusion processes are involved and therefore the activation energy required for subsurface migration is slightly different depending on whether the adsorption of hydrogen or deuterium is considered.<sup>15</sup>

Our results also shed light on the question about the desorption temperature of subsurface H atoms, a still controversial subject in the literature on Pd(110). Whereas some authors have claimed that the subsurface species should desorb in the  $\alpha$  states, the results presented in Figs. 6 and 10 demonstrate that subsurface H atoms actually desorb in the  $\beta_1$  state, as previously suggested by Norton *et al.*<sup>12</sup> for the H/Pd(110) system. Note also that, although the  $\beta_1$  and  $\alpha$  states can be populated at 130 K after high H doses, our current results demonstrate that, by heating the (2 $\times$ 1)3H phase to 220 K, the  $\beta_1$  state (subsurface H atoms) can be populated before the  $\beta_2$  state (chemisorbed H atoms) is saturated. This means that at 220 K the more stable configuration is the one with 0.5 ML chemisorbed H atoms and the rest occupying subsurface sites.

Concerning the HREELS results, the fact that the 120 meV peak saturates only after 10 L exposure (whereas the surface corrugation does not change from  $\sim 0.6$  L on as revealed by HAS) suggests that this peak is strongly affected by the presence of H atoms below the surface. When the surface is saturated with 1 ML the tetrahedral site exhibits a distance from the adsorption sites that is with 0.98 Å (threefold site) and 1.59 Å (fourfold site) very small. Only the octahedral site between the second and third layers shows a distance from the adsorption sites that is nearly the same as the smallest distance observed for two hydrogen atoms in the bulk.<sup>45</sup> Therefore it seems reasonable to assume that the octahedral site below the surface is occupied. On Pd(110) the situation is different since the octahedral site is closer to the adsorption sites. The pairing-row reconstruction leads to the appearance of a more open surface and subsurface octahedral sites in the second layer may also be accessed. This could explain why on Pd(110) no increase of the dynamic dipole moment associated with the threefold adsorption site has been observed.

## ACKNOWLEDGMENTS

The authors wish to thank Ch. Roth for technical assistance. D.F. gratefully acknowledges support by the Deutsche Forschungsgemeinschaft.

- <sup>1</sup>E. Wicke and H. Brodowsky, in *Hydrogen in Metals*, edited by G. Alefeld and J. Voelkl, Topics in Applied Physics Vol. 29 (Springer, Berlin, 1978), Vol. 2, p. 73.
- <sup>2</sup>W. Zhong, Y. Cai, and D. Tománek, *Nature (London)* **362**, 435 (1993).
- <sup>3</sup>J. N. Huiberts, R. Griessen, J. H. Rector, R. J. Wijngaarden, J. P. Dekker, D. G. de Groot, and N. J. Koeman, *Nature (London)* **380**, 231 (1996).
- <sup>4</sup>R. J. Behm, K. Christmann, and G. Ertl, *Surf. Sci.* **99**, 320 (1980).
- <sup>5</sup>H. Okuyama, W. Siga, N. Takagi, M. Nishijima, and T. Aruga, *Surf. Sci.* **401**, 344 (1998).
- <sup>6</sup>T. Engel and H. Kuipers, *Surf. Sci.* **90**, 162 (1979).
- <sup>7</sup>T. E. Felner, S. M. Foiles, M. S. Daw, and R. H. Stulen, *Surf. Sci.* **171**, L379 (1986).

- <sup>8</sup>G. D. Kubiak and R. H. Stulen, *J. Vac. Sci. Technol. A* **4**, 1427 (1986).
- <sup>9</sup>R. J. Behm, V. Penka, M. G. Cattania, K. Christmann, and G. Ertl, *J. Chem. Phys.* **78**, 7486 (1983).
- <sup>10</sup>K. H. Rieder, M. Baumberger, and W. Stocker, *Phys. Rev. Lett.* **51**, 1799 (1983).
- <sup>11</sup>M. Baumberger, W. Stocker, and K. H. Rieder, *Appl. Phys. A: Solids Surf.* **41**, 151 (1986).
- <sup>12</sup>J.-W. He, D. A. Harrington, K. Griffiths, and P. R. Norton, *Surf. Sci.* **198**, 413 (1988).
- <sup>13</sup>W. Dong, V. Ledentu, P. Sautet, G. Kresse, and J. Hafner, *Surf. Sci.* **377-379**, 56 (1997).
- <sup>14</sup>D. Fariás, H. Tröger, M. Patting, and K. H. Rieder, *Surf. Sci.* **352-354**, 155 (1996).
- <sup>15</sup>D. Fariás, M. Patting, and K. H. Rieder, *Phys. Status Solidi A* **159**, 255 (1997).
- <sup>16</sup>P. Schilbe, D. Fariás, and K. H. Rieder, *Surf. Rev. Lett.* **5**, 473 (1998).
- <sup>17</sup>T. Engel and K. H. Rieder, *Surf. Sci.* **109**, 40 (1981).
- <sup>18</sup>P. Schilbe, S. Siebentritt, R. Poes, and K. H. Rieder, *Surf. Sci.* **360**, 157 (1996).
- <sup>19</sup>J.-W. He, U. Memmert, K. Griffiths, and P. R. Norton, *J. Chem. Phys.* **90**, 5082 (1989).
- <sup>20</sup>K. H. Rieder, *Phys. Rev. B* **27**, 7799 (1983).
- <sup>21</sup>K. Christman, *Mol. Phys.* **66**, 1 (1989).
- <sup>22</sup>T. Engel and K. H. Rieder, in *Structural Studies of Surfaces*, Springer Tracts in Modern Physics Vol. 91 (Springer, Berlin, 1982), p. 55.
- <sup>23</sup>W. Frie, L. Hammer, and K. Heinz (unpublished).
- <sup>24</sup>G. E. Gdowski, T. E. Felner, and R. H. Stulen, *Surf. Sci.* **181**, L147 (1987).
- <sup>25</sup>H. Conrad, G. Ertl, and E. E. Latta, *Surf. Sci.* **41**, 435 (1974).
- <sup>26</sup>M. Mavrikakis, J. W. Schwank, and J. L. Gland, *J. Chem. Phys.* **105**, 8398 (1997).
- <sup>27</sup>M. G. Cattania, V. Penka, R. J. Behm, K. Christmann, and G. Ertl, *Surf. Sci.* **126**, 382 (1983).
- <sup>28</sup>K. Christmann, *Surf. Sci. Rep.* **9**, 1 (1988).
- <sup>29</sup>P. A. Redhead, *Vacuum* **12**, 203 (1962).
- <sup>30</sup>E. Habenschaden and J. Küppers, *Surf. Sci.* **138**, L147 (1984).
- <sup>31</sup>A. D. Johnson, K. J. Maynard, S. P. Daley, Q. Y. Yang, and S. T. Ceyer, *Phys. Rev. Lett.* **67**, 927 (1991).
- <sup>32</sup>T. H. Ellis and M. Morin, *Surf. Sci.* **216**, L351 (1989).
- <sup>33</sup>U. Muschiol, P. K. Schmidt, and K. Christmann, *Surf. Sci.* **395**, 182 (1998).
- <sup>34</sup>C. Nyberg and C. G. Tengstal, *Solid State Commun.* **44**, 251 (1982).
- <sup>35</sup>H. Conrad, M. E. Kordesch, W. Stenzel, M. Sunjic, and B. Trninc-Radja, *Surf. Sci.* **178**, 578 (1986).
- <sup>36</sup>H. Conrad, M. E. Kordesch, W. Stenzel, and M. Sunjic, *J. Vac. Sci. Technol. A* **5**, 452 (1987).
- <sup>37</sup>H. Conrad, M. E. Kordesch, R. Scala, and W. Stenzel, *J. Electron Spectrosc. Relat. Phenom.* **38**, 289 (1986).
- <sup>38</sup>D. Fariás, S. Siebentritt, R. Apel, R. Poes, and K. H. Rieder, *J. Chem. Phys.* **106**, 8254 (1997).
- <sup>39</sup>S. W. Rick and J. D. Doll, *Surf. Sci.* **302**, L305 (1994).
- <sup>40</sup>J. J. Rush, J. M. Rowe, and D. Richter, *Z. Phys. B* **55**, 283 (1984).
- <sup>41</sup>J. M. Nicol, *Phys. Rev. B* **36**, 9315 (1987).
- <sup>42</sup>M. Patting, D. Fariás, and K. H. Rieder (unpublished).
- <sup>43</sup>D. Hennig, S. Wilke, R. Löber, and M. Methfessel, *Surf. Sci.* **287/288**, 89 (1993).
- <sup>44</sup>C. Nyberg and L. Westerlund, *Surf. Sci.* **256**, 9 (1991).
- <sup>45</sup>A. C. Switendick, in *Hydrogen in Metals*, edited by G. Alefeld and J. Voelkl, Topics in Applied Physics Vol. 28 (Springer, Berlin, 1978), Vol. 1, p. 106.
- <sup>46</sup>O. B. Christensen, P. D. Ditlevsen, K. W. Jacobsen, P. Stotze, O. H. Nielsen, and J. K. Nørskov, *Phys. Rev. B* **40**, 1993 (1989).
- <sup>47</sup>D. Fariás, M. Patting, and K. H. Rieder, *Surf. Sci.* **385**, 115 (1997).